

1
2
3
4
5
6
7
8
9
10
11
12
13
14
15
16
17
18
19
20
21
22
23

Near real-time field measurements of $\delta^{13}\text{C}$ in CO_2 from volcanoes

John Stix, Gregor Lucic², and Kalina Malowany³

Department of Earth and Planetary Sciences, McGill University, 3450 University Street,
Montreal, Quebec H3A 0E8, Canada. Email: stix@eps.mcgill.ca

²Now at: Picarro Inc., 3105 Patrick Henry Drive, Santa Clara, CA 95054, USA

³Now at: Core6 Environmental, 777 Hornby Street, Suite 1410, Vancouver, BC V6Z 1S4,
Canada

24 Abstract

25

26 This paper describes the operation and application of a portable cavity ring-down
27 spectrometer (CRDS) designed to measure the isotopic composition of carbon dioxide.
28 The instrument is capable of measuring $\delta^{13}\text{C}$ for CO_2 concentrations ranging from
29 atmospheric (400 ppm) to 100%, at precisions and accuracies that are comparable to
30 laboratory-based gas source mass spectrometers. This flexibility and portability are ideal
31 for applications on active volcanoes, and it is now possible to obtain isotopic
32 measurements on a near real-time basis. We show applications of the CRDS for soil
33 gases on volcanoes and in calderas, for characterizing the isotopic composition of a
34 volcanic plume, and for measuring the temporal variability of $\delta^{13}\text{C}$ in the atmosphere.
35 Future directions hold the potential to use volcanic gas isotopes for monitoring purposes,
36 and to combine different isotopic systems to reveal the source or sources of gas.

37

38

39 1. Introduction

40

41 Volcanic gases provide important clues to volcanic activity. Not only can gases
42 indicate the state of unrest of an active volcano, they also reveal the ultimate source or
43 sources of the gas. In this regard, both gas concentrations and stable isotope signatures of
44 species such as H_2O and CO_2 play an important role. Coupled with other monitoring tools
45 such as seismic and geodetic monitoring, gas data yield important insights into a
46 volcano's activity, including whether the system is accelerating or decelerating in terms

47 of restlessness. Sometimes anomalous emanations of gas are the first signs that a volcano
48 is reawakening, and both increases and decreases in gas output, e.g., sulfur dioxides
49 fluxes, have been documented prior to explosive eruptions (Daag et al. 1996; Zapata G et
50 al. 1997; Conde et al. 2014).

51 In the past 20 years, significant advances have been made in studying and
52 monitoring volcanic gases. Small, inexpensive mini-DOAS and FLYSPEC instruments
53 have replaced the COSPEC for SO₂ flux measurements, which can be made from a
54 variety of mobile and stationary configurations including automated data collection on a
55 real-time basis (e.g., Galle et al. 2003; Edmonds et al. 2003; Horton et al. 2006). FTIR
56 remote sensing measurements of plumes and craters have successfully characterized
57 multiple gas species; in favorable circumstances a full spectrum of gas species can be
58 identified and quantified (e.g., Oppenheimer et al. 2006). Similarly, Multi-GAS
59 instruments are able to measure a variety of gas species in situ (Shinohara 2005); gas
60 ratios can be easily derived from these measurements, with the CO₂/SO₂ ratio proving
61 especially useful in tracking unrest (e.g., Aiuppa et al. 2007; de Moor et al. 2016).

62 Here we report on a new field-based approach for measuring the isotopic
63 concentration of carbon dioxide emanating from volcanoes. The instrument deployed is a
64 cavity ring-down spectrometer (CRDS) with precisions and accuracies that are
65 comparable to conventional laboratory mass spectrometers. The principal advance is that
66 we are able to make isotopic measurements on a near real-time basis in the field, allowing
67 us to rapidly identify and map zones of magmatic CO₂. Typically, gas samples are
68 collected and isotopic measurements made the same day, thereby decreasing the wait
69 time for analysis and allowing sampling flexibility during a field campaign. The

70 instrument can be deployed in a number of configurations, and together with isotope ratio
71 infrared spectrometry (IRIS) (Rizzo et al. 2014, 2015; Fischer and Lopez 2016), it is the
72 only practical means of measuring the carbon isotopic composition of a degassing plume.

73

74

75 2. Principle of operation

76

77 The Picarro G1101-i CRDS exploits the near-infrared absorption of carbon's two
78 isotopologues (^{13}C and ^{12}C). A single frequency laser diode produces a beam that enters
79 the vacuum filled cavity with a unique wavelength that corresponds to the vibrational
80 frequency of the target isotopologue. Within the cavity, the beam is reflected among three
81 mirrors over an effective pathlength of > 20 km, increasing in intensity over time. When
82 a threshold is reached, the sample gas is introduced and the intensity of the light
83 decreases with time due to the resonant absorption of energy by the target molecule (e.g.,
84 $^{12}\text{C}^{16}\text{O}_2$). The 'ring-down' time is the time required for the light intensity to drop to
85 starting levels. Isotope concentrations are reported every ten seconds and are derived by
86 comparing the difference in ring-down times between a sample-filled cavity and an
87 empty one. This comparative method produces precise and robust quantitative
88 measurements, independent of fluctuations in laser intensity and absolute laser power
89 (Picarro Inc. 2015).

90 In practical terms, our CRDS comprises two components, one a data acquisition
91 module (DAS) which houses the cavity and the other a power supply and vacuum pump
92 module (CPVU). More recent versions comprise a single module. Together, the two

93 components weigh ~34 kg, and their footprint is similar to that of a large desktop
94 computer (Fig. 1). The unit needs only electricity with a maximum power requirement of
95 375 watts. We generally run the instrument with an uninterruptible power supply (UPS)
96 attached to house current, to ensure stable power and avoid any cuts in electricity to the
97 instrument.

98

99

100 3. Calibration

101

102 Under controlled laboratory conditions, our Picarro instrument can easily achieve
103 sub-per mil precision. CO₂ gas standards run in the lab at 1000-3000 ppm concentration
104 levels show nominal reproducibilities on the order of 0.3-0.5 per mil, but multiple
105 analyses of individual samples show that the true reproducibility can approach 0.1 per mil.
106 The nominal reproducibility is simply the standard deviation on the average of multiple
107 measurements of a single sample, while the true reproducibility is based on averaging
108 multiple samples of a standard. During field deployments, 0.5 per mil or better
109 reproducibility at 1000-3000 ppm CO₂ is achievable. At atmospheric conditions (~400
110 ppm), the nominal error is typically ~1 per mil, but repeat analyses of standards
111 demonstrate that the actual error is again better than this.

112 Prior to a field deployment, the instrument is calibrated in the lab using a series of
113 four in-house standard gases with various isotopic compositions from -43‰ to -11.4‰
114 that have been calibrated independently by gas source mass spectrometry using a series
115 of gas standards referenced to internationally accepted reference materials. For greatest

116 precision and accuracy, we try to maintain a similar CO₂ concentration whenever
117 possible for both standards and samples. This is because there can be a small
118 concentration-dependent variation for $\delta^{13}\text{C}$, even though this effect is corrected by the
119 Picarro algorithm. We generally do our calibrations at 1000 ppm CO₂ for good
120 reproducibility, but concentrations of 2000 or 3000 ppm also can be used (Fig. 2). To
121 maintain similar CO₂ concentrations, we do sample dilutions using air in which the CO₂
122 has been removed by an ascarite (NaOH) filter. Calibrations also can be done at
123 atmospheric levels, i.e., 400 ppm, but the reproducibility is slightly degraded at these
124 lower concentrations. In the field prior to commencing measurements, we check the lab
125 calibration with our standards and redo the calibration if required with three of our four
126 gas standards. Thereafter we run our -15.6 per mil standard interspersed with our
127 unknown samples. The standard is always run at the same concentration (e.g., 1000 ppm)
128 as the samples. Typically, these calibrations are stable for days to weeks at a time. If the
129 standard differs by more than 1 per mil from the accepted value, we redo the full
130 calibration.

131 In the early stages of development and deployment, we were cognizant of the
132 need to demonstrate accuracy and precision of our CRDS measurements. Hence we took
133 special care to measure selected standards and samples on both our Picarro instrument
134 and also on a Finnigan MAT gas source mass spectrometer paired to a gas chromatograph
135 combustion interface with a continuous flow-through system at the University of Toronto.
136 Figure 3 is a plot showing measurements of the same samples made by the two different
137 types of measurements; the correspondence is excellent, demonstrating the viability of
138 the CRDS technique.

139

140

141 4. Interferences

142

143 Under normal atmospheric conditions, the only interferences that the CRDS
144 experiences are those from water vapor (Rella et al. 2013) and methane (Vogel et al.
145 2013), which are accounted for and corrected by the instrument's hardware and software.
146 Variable CO₂ concentrations from 400 to 3000 ppm are also accounted for when δ¹³C is
147 being measured. Nevertheless, we generally make our measurements at a fixed
148 concentration value, as explained above, to minimize any residual concentration-
149 dependent effects.

150 In gases containing hydrogen sulfide, we have observed a significant effect of this
151 species upon the δ¹³C signal (Malowany et al. 2015). In essence, the presence of H₂S
152 imparts a strongly negative value to δ¹³C as a result of H₂S interference primarily upon
153 the ¹³C isotope (Fig. 4). As a result, the CRDS δ¹³C measurement is strongly dependent
154 upon both H₂S and CO₂ concentrations, being most severe at low CO₂ and high H₂S. For
155 example, at 1000 ppm CO₂ and ~30 ppb H₂S, the negative δ¹³C shift is ~ -1 per mil. This
156 isotopic shift is observed over the entire operating range of the instrument (400 – 3000
157 ppm CO₂) and for H₂S concentrations in excess of 1 ppb (Malownany et al. 2015).

158 The simplest and most effective way to deal with this interference is to remove it,
159 and we do this by using a metal scrub, typically copper, which reacts with the hydrogen
160 sulfide to form copper sulfide by the reaction $2\text{H}_2\text{S} + 2\text{Cu} + \text{O}_2 \rightarrow 2\text{CuS} + 2\text{H}_2\text{O}$. In
161 practical terms, we use a 10-20 cm length of 1/4-inch diameter copper tubing that is filled

162 with copper filings in order to enhance reactivity by increased surface area (Fig. 5); our
163 experiments suggest that not all H₂S is removed with only the copper tube or copper
164 filings alone (Malowany et al. 2015) The copper tubes are utility grade, the copper filings
165 are CHEM.57B grade “B”, and both contain small amounts of other metals. We use these
166 copper tubes both in field sampling from vents and fumaroles, and also during the CRDS
167 analysis, so that the gas has passed through this double set of filters before entering the
168 instrument. The copper filters have no measurable effect on the carbon isotope
169 composition or gas concentrations (Malowany et al. 2015). The tubes and filings need to
170 be replaced periodically before they have reacted fully with the H₂S. This can be assessed
171 visually, as the copper turns black during reaction with H₂S. Using this approach ensures
172 that the gas is free of hydrogen sulfide during isotopic analysis of the CO₂. In volcanic
173 environments that typically have H₂S present, this procedure is essential to obtain
174 accurate and precise CRDS measurements.

175

176

177 5. Sampling and measurement

178

179 When sampling in the field, we pump the gas into 1000 ml ALTEF or Tedlar
180 sampling bags (Fig. 6). As we pump the gas, we also measure its CO₂ concentration using
181 a portable infrared CO₂ instrument. If the gas exceeds 3000 ppm CO₂, it is too
182 concentrated for the CRDS, so we dilute it in the field. For example, if the gas is 100%
183 CO₂, we inject 1 ml of the gas into a sampling bag prefilled with 1000 ml air that has
184 been scrubbed of CO₂ by passing it through an ascarite filter in the lab or hotel room (Fig.

185 7). This dilution produces a gas with ~1000 ppm CO₂, suitable for analysis by the CRDS.
186 In this situation, we run all our samples including unknowns and standards at 1000 ppm
187 CO₂ for maximum consistency. If the gas is less than 3000 ppm CO₂, we can either
188 sample and measure it without dilution, or do a small dilution to obtain 1000 ppm.

189 In general, it is a good idea to take duplicate samples from time to time for later
190 analysis by conventional gas source mass spectrometry. This provides a further check of
191 accuracy for the CRDS. To do this, we take a 50-ml sample from a gas bag, placing this
192 volume in a pressurized 30 ml anaerobic culture tube containing 5 µl of HgCl₂ to prevent
193 any bacterial production that might affect the δ¹³C value between sampling and analysis
194 (typically several weeks to months) (Fig. 8a) (Oremland et al. 1987).

195 Our general protocol is to collect gas samples during the day, then analyze them
196 in the evening. This protocol minimizes the time during which gas can diffuse into or out
197 of the bag. In this manner, we process approximately 10 samples each day. Prior to
198 analyzing our samples, we check the calibration of the CRDS by running 3-4 of our in-
199 house CO₂ gas standards spanning a range of isotope compositions. If the calibration is
200 accurate, we can analyze our samples; if it is not, we recalibrate the CRDS. We transport
201 our standard gases to the field in 210-ml anaerobic media bottles (Fig. 8b). This method
202 obviates the need for compressed gases and associated paraphernalia, and we have
203 sufficient standard gas to run periodically, interspersed with our samples, as a check on
204 accuracy and precision.

205 To analyze our samples is a straightforward procedure. We attach the gas bag
206 directly to the instrument which pumps gas into the analyzer at a rate of ~0.1 l/min. An
207 analysis time of ~10-15 minutes is generally sufficient; the data are normally averaged

208 over this time period, except for the first several minutes which are not used because the
209 CO₂ concentrations entering the CRDS are changing from atmospheric to those of the
210 sampling bag (Fig. 9). Once the analysis is finished, the sample bag is disconnected from
211 the instrument, the CRDS re-equilibrates to atmospheric conditions for a few minutes,
212 and then the next sample bag is attached to the instrument for the subsequent analysis. A
213 CO₂ gas standard is run after 5-10 samples, always at similar CO₂ concentrations as the
214 samples, as a check of accuracy and precision.

215

216

217 6. Applications

218

219 Because the CRDS is portable, it can be easily used in the field to collect isotopic
220 data of high precision and accuracy. Its portability and field use are advantageous when a
221 field campaign needs to be adjusted or modified to a changing situation. For example, if a
222 particular location becomes inaccessible, samples can be collected elsewhere and
223 analyzed promptly. Below we summarize three useful applications of the CRDS at
224 volcanoes.

225

226 Isotopic characterization of soil gases

227

228 Soil gases in volcanic areas are commonly rich in carbon dioxide, and the gas is
229 typically a mixture of deep, biogenic, and atmospheric CO₂. Studying soil gases in
230 calderas can be particularly fruitful, as magmatic or hydrothermal CO₂ can reveal

231 subsurface fault structures which serve to focus gas flow. At Long Valley caldera our
232 goal was to extend the work of Bergfeld et al. (2006), in order to understand the role and
233 interplay of regional faults and caldera faults in influencing the release of magmatic CO₂
234 gas. To do this, we sampled soil gases and fumaroles in and around the caldera, targeting
235 key areas such as the caldera margin, the south moat of the caldera which is very active
236 seismically, and the resurgent dome which has been uplifted by nearly one meter since
237 the early 1980's. In order to characterize the magmatic CO₂ emissions, we also needed to
238 identify other sources of CO₂, namely biogenic and atmospheric (Lucic et al. 2015). The
239 samples from the southern margin of the resurgent dome reveal a dominantly magmatic
240 character, consistent with the volcanic unrest in this sector of the caldera. A number of
241 these points plot in the mixing field, showing variable contributions of the three end-
242 members (Lucic et al. 2015). This example demonstrates the importance of conducting a
243 comprehensive characterization of the CO₂ budget of a particular site, so that subtle
244 differences in mixing can be identified and interpreted.

245

246 Isotopic characterization of volcanic plumes

247

248 Characterizing the isotopic character of a volcanic plume can yield significant
249 insight regarding the source of the CO₂. Monitoring the isotopic composition of the
250 plume over time can provide invaluable monitoring data in terms of processes such as
251 magma degassing and magma replenishment within or beneath the volcano. Chiodini et
252 al. (2011) pioneered this approach on a number of Italian volcanoes, and more recently
253 several studies used isotope ratio infrared spectrometry (IRIS) to isotopically characterize

254 plumes (Rizzo et al. 2014, 2015; Fischer and Lopez 2016). We applied the CRDS to
255 measure $\delta^{13}\text{C}$ in the plume of Turrialba volcano in Costa Rica. Turrialba has shown
256 escalating activity since the late 1990's, and the volcano is currently in a state of
257 heightened unrest. Gases have become less hydrothermal and more magmatic over time
258 (Moussallam et al. 2014; De Moor et al. 2016), and SO_2 fluxes are high and variable. In
259 late 2014 and 2015, solid juvenile material was erupted for the first time (Global
260 Volcanism Program, 2015). Our goal at Turrialba was to characterize the isotopic
261 character of the CO_2 being emitted from the volcano through soil gases, fumaroles, and
262 high-temperature vents. A primary objective was an attempt to characterize the volcano's
263 plume for its carbon isotopic signature. The CRDS is an ideal instrument for isotopic
264 analysis of the plume for two reasons. First, a number of gas samples can be collected
265 fairly quickly in the plume, then analyzed immediately afterward. Second, the sub per mil
266 precision of the CRDS allows us to discriminate between samples with small isotopic
267 differences. At Turrialba, this entailed taking multiple samples from within the plume at
268 CO_2 concentrations of 400-800 ppm and then analyzing them on the CRDS. Because the
269 plume is diluted significantly by atmospheric CO_2 , it was necessary to conduct a detailed
270 mixing model for the plume (Malowany et al. 2017). Extrapolation of the plume data
271 from the atmospheric end-member through the data points from the plume reveals that
272 the magmatic end-member has a $\delta^{13}\text{C}$ value of -2.9 ± 0.5 per mil, which is similar to
273 other low-temperature fumaroles and soil gases in and around the crater. By contrast, the
274 high-temperature 2012 vent ($\geq 480^\circ \text{C}$) is offset to slightly lighter values (-4.4 per mil).
275 These results reveal the complex and heterogeneous isotopic character of CO_2 emissions
276 at Turrialba.

277

278 $\delta^{13}\text{C}$ of atmospheric CO_2

279

280 The CRDS is effective at accurately measuring sub per mil variations in
281 atmospheric CO_2 concentrations and isotopic compositions (Vogel et al. 2013). Global
282 atmospheric CO_2 concentrations currently are around 400 ppm and rising, with isotopic
283 concentrations of -8.2‰ and decreasing (Cuntz 2011). Anthropogenic pollution can
284 influence the atmospheric CO_2 concentration and $\delta^{13}\text{C}$ signal. Furthermore, diurnal
285 variations of CO_2 concentration and $\delta^{13}\text{C}$ arise from photosynthetic and respiratory
286 activity of plants, causing variations in the isotopic signal from local vegetation (Lloyd et
287 al. 1996). At Turrialba volcano, variations in the atmospheric isotopic composition were
288 approximately 2 per mil due to photosynthesis of the surrounding rainforest (Malowany
289 et al. 2017). The most enriched values occurred at mid-day, resulting from the
290 preferential uptake of ^{12}C when photosynthetic activities were at their maximum.
291 Characterizing and understanding these variations in ambient atmosphere are important
292 for the implementation of mixing plots among atmospheric, volcanic and biogenic
293 endmembers. The CRDS is well equipped to measure these subtle changes in
294 atmospheric $\delta^{13}\text{C}$, and thus is highly advantageous for detailed studies addressing the
295 interaction of multiple carbon components.

296

297

298 7. Future directions

299

300 The isotopic character of CO₂ at a volcano is a useful measurement that can now
301 be done on a routine basis during field deployments. Characterizing the carbon isotopic
302 character of a volcano provides a basis and baseline to understand its CO₂ emissions and
303 source or sources. The isotopic signal may vary with time, and this could signify a
304 change in the volcano's condition and state of activity. For example, δ¹³C values that
305 become increasingly negative could signify a progressively degassing magma, a
306 decreasing hydrothermal and increasing magmatic component, and/or an increased
307 biogenic component. Isotopic values which become more positive could be indicative of
308 an increasing crustal component or the arrival of new magma rich in CO₂ (see Malowany
309 et al. 2017). Such variations are potentially useful for volcano monitoring.

310 A particularly interesting application well suited for CRDS instruments is the
311 measurement of volcanic plumes, as we have done at Turrialba. Such measurements hold
312 promise for monitoring purposes. It is possible that isotopic shifts occur in open systems,
313 such as when CO₂ is transported from deep crustal or mantle environments into the
314 shallow plumbing system of a volcano. Coupled with Multi-GAS measurements of C/S,
315 determining the carbon isotopic composition of the plume on a regular or continuous
316 basis could reveal significant variations with time that correlate with eruptive activity.
317 For such isotopic measurements to be robust and useful, it is essential that (a) plume
318 samples are accurately and precisely measured for both CO₂ concentration and δ¹³C, and
319 (b) the atmospheric end-member is well characterized, especially if its CO₂ concentration
320 and δ¹³C value are not constant as a function of time.

321 Chiodini et al. (2008) pioneered the integration of CO₂ fluxes and isotopes in soil
322 gas. We took this approach at Cerro Negro volcano in Nicaragua. Samples with high CO₂

323 fluxes invariably had a magmatic isotopic character of -2 to -5 per mil, while lower-flux
324 samples showed an increasing influence of biogenic CO₂ (Lucic et al. 2014). In this case
325 we did our carbon isotope measurements by gas source mass spectrometry after the field
326 campaign. However, this example illustrates the potential of simultaneous deployment of
327 the CRDS coupled with CO₂ flux measurements. This field-based approach is the ideal
328 means of fully characterizing the CO₂ output of a volcano, providing crucial information
329 on both the strength and the source of the CO₂ signal. The data which are collected are
330 nearly real-time, allowing a rapid and highly detailed characterization of the CO₂
331 emissions. Furthermore, specific zones can be targeted at high spatial and temporal
332 resolutions.

333 An increasing number of manufacturers are producing CRDS and related
334 instruments that are field-deployable to measure the isotopic character of CO₂ and other
335 gases at active volcanoes. The procedures and applications that we have highlighted in
336 this paper should be applicable for these new developments. Furthermore, this advance
337 provides new possibilities for volcano monitoring. For example, a series of CRDS
338 instruments could be installed permanently at a volcano, making continuous and
339 automated $\delta^{13}\text{C}$ measurements which are telemetered to an observatory on a true real-
340 time basis. Since many volcanoes are dangerous to sample directly, this type of remote
341 monitoring can be highly advantageous. Field-based approaches also can be taken using
342 hydrogen and oxygen isotopes for fluids and gases. When coupled with the CO₂
343 measurements, these additional isotopic systems can provide more detailed insight
344 regarding sources and degassing mechanisms. We are excited about exploiting these new
345 opportunities.

346

347

348 Acknowledgements

349

350 We are most grateful to the staff at Picarro Inc. for their continued assistance and interest
351 in our applications, most notably Aaron Van Pelt, Mike Ahern, Danthu Vu, and Linda
352 Huynh. Aaron has been a steadfast and enthusiastic supporter of using this technology for
353 applications on active volcanoes. Maarten de Moor has provided crucial scientific and
354 logistical advice at Turrialba. Boswell Wing of McGill University has helped us
355 considerably in a number of ways, extending his extensive isotopic knowledge and
356 perceptive insight to help us resolve a variety of issues. Barbara Sherwood Lollar,
357 Georges Lacrampe-Couloume, and Katrina Chu of the University of Toronto have
358 provided fundamentally important scientific and technical input into cross-calibration of
359 our Picarro CRDS with their gas source mass spectrometers. We thank one anonymous
360 reviewer, Taryn Lopez, and the editor Toby Fischer for helpful comments and
361 suggestions that improved the paper. We acknowledge ongoing support from the Natural
362 Sciences and Engineering Research Council of Canada for this research through
363 Discovery, Accelerator, and Create grants to JS.

364

365

366 References cited

367

368 Aiuppa A, Moretti R, Federico C, Giudice G, Gurrieri S, Liuzzo M, Papale P, Shinohara
369 H, Valenza M (2007) Forecasting Etna eruptions by real-time observation of volcanic
370 gas composition. *Geology* 35:1115-1118

371 Bergfeld D, Evans WC, Howle JF, Farrar CD (2006) Carbon dioxide emissions from
372 vegetation-kill zones around the resurgent dome of Long Valley Caldera, eastern
373 California, USA, *J Volcanol Geotherm Res* 152:140–156

374 Chiodini G, Caliro S, Cardellini C, Avino R, Granieri D, Schmidt A (2008) Carbon
375 isotopic composition of soil CO₂ efflux, a powerful method to discriminate different
376 sources feeding soil CO₂ degassing in volcanic-hydrothermal areas. *Earth Planet Sci*
377 *Lett* 274:372–379

378 Chiodini G, Caliro S, Aiuppa A, Avino R, Granieri D, Moretti R, Parello F (2011) First
379 ¹³C/¹²C isotopic characterization of volcanic plume CO₂. *Bull Volcanol* 73:531–542

380 Conde V, Bredemeyer S, Duarte E, Pacheco JF, Miranda S, Galle B, Hansteen TH (2014)
381 SO₂ degassing from Turrialba volcano linked to seismic signatures during the period
382 2008-2012. *Int J Earth Sci* 103:1983-1998

383 Cuntz M (2011) Carbon cycle: a dent in carbon's gold standard. *Nature* 477:547-548

384 Daag AS, Tubianosa BS, Newhall CG, Tuñgol NM, Javier D, Dolan MT, Reyes PJD,
385 Arboleda RA, Martinez MML, Regalado MTM (1996) Monitoring sulfur dioxide
386 emission at Mount Pinatubo. In: Newhall CG, Punongbayan RS (eds) *Fire and mud,*
387 *eruptions and lahars of Mount Pinatubo, Philippines.* Philippine Institute of
388 *Volcanology and Seismology, Quezon City, University of Washington Press, Seattle,*
389 *pp 409-414*

390 De Moor JM, Aiuppa A, Avarad G, Wehrmann H, Dunbar N, Muller C, Tamburello G,
391 Giudice G, Liuzzo M, Moretti R, Conde V, Galle B (2016) Turmoil at Turrialba
392 volcano (Costa Rica): degassing and eruptive processes inferred from high-frequency
393 gas monitoring. *J Geophys Res* 121:5761-5775, doi:10.1002/2016JB013150

394 Edmonds M, Herd RA, Galle B, Oppenheimer CM (2003) Automated, high time
395 resolution measurements of SO₂ flux at Soufrière Hills volcano, Montserrat. *Bull*
396 *Volcanol* 65:578-586

397 Fischer TP, Lopez TM (2016) First airborne samples of a volcanic plume for $\delta^{13}\text{C}$ of CO₂
398 determinations. *Geophys Res Lett* 43:3272-3279, doi:10.1002/2016GL068499

399 Galle B, Oppenheimer C, Geyer A, McGonigle AJS, Edmonds M, Horrocks L (2003) A
400 miniaturised ultraviolet spectrometer for remote sensing of SO₂ fluxes: A new tool for
401 volcano surveillance. *J Volcanol Geotherm Res* 119:241–254

402 Global Volcanism Program (2015) Report on Turrialba (Costa Rica). In: Wunderman R
403 (ed) *Bulletin of the Global Volcanism Network*, Smithsonian Institution 40:4

404 Horton KA, Williams-Jones G, Garbeil H, Elias T, Sutton AJ, Mouginiis-Mark P, Porter
405 JN, Clegg S (2006) Real-time measurement of volcanic SO₂ emissions: validation of a
406 new UV correlation spectrometer (FLYSPEC). *Bull Volcanol* 68:323-327

407 Lloyd J, Kruijt B, Hollinger DY, Grace J, Francey RJ, Wong SC, Kelliher FM, Miranda
408 AC, Farquhar GD, Gash JH, Vygodskaya NN (1996) Vegetation effects on the
409 isotopic composition of atmospheric CO₂ at local and regional scales: theoretical
410 aspects and a comparison between rain forest in Amazonia and a boreal forest in
411 Siberia. *Funct Plant Biol* 23:371–399

412 Lucic G, Stix J, Sherwood Lollar B, Lacrampe-Couloume G, Muñoz A, Ibarra C M
413 (2014) The degassing character of a young volcanic center: Cerro Negro, Nicaragua.
414 Bull Volcanol 76:850, doi:10.1007/s00445-014-0850-6

415 Lucic G, Stix J, Wing B (2015) Structural controls on the emission of magmatic carbon
416 dioxide gas, Long Valley Caldera, USA. J Geophys Res 120:2262-2278,
417 doi:10.1002/2014JB011760

418 Malowany K, Stix J, Van Pelt A, Lucic G (2015) H₂S interference on CO₂ isotopic
419 measurements using a Picarro G1101-i cavity ring-down spectrometer. Atmos Meas
420 Tech 8:4075-4082

421 Malowany K, Stix J, de Moor M, Sherwood Lollar B, Chu K, Lacrampe-Couloume G
422 (2017) Carbon isotope systematics of Turrialba volcano, Costa Rica, using a portable
423 cavity ring-down spectrometer. Geochem Geophys Geosyst, in press

424 Moussallam Y, Peters N, Ramírez C, Oppenheimer C, Aiuppa A, Giudice G (2014)
425 Characterisation of the magmatic signature in gas emissions from Turrialba volcano,
426 Costa Rica. Solid Earth 5:1341–1350, doi:10.5194/se-5-1341-2014

427 Oppenheimer C, Bani P, Calkins JA, Burton MR, Sawyer GM (2006) Rapid FTIR
428 sensing of volcanic gases released by strombolian explosions at Yasur volcano,
429 Vanuatu. Appl Phys B 85:453-460

430 Oremland RS, Miller LG, Whiticar MJ (1987) Sources and flux of natural gases from
431 Mono Lake, California. Geochim Cosmochim Acta 51:2915-2929

432 Picarro Inc. (2015) Cavity ring-down spectroscopy (CRDS). Picarro
433 Inc. http://www.picarro.com/technology/cavity_ring_down_spectroscopy. Accessed
434 15 July 2015 2015

435 Rella CW, Chen H, Andrews AE, Filges A, Gerbig C, Hatakka J, Karion A, Miles NL,
436 Richardson SJ, Steinbacher M, Sweeney C, Wastine B, Zellweger C (2013) High
437 accuracy measurements of dry mole fractions of carbon dioxide and methane in humid
438 air. *Atmos Meas Techn* 6:837–860, doi:10.5194/amt-6-837-2013

439 Rizzo A, Jost H, Caracausi A, Paonita A, Liotta M, Martelli M (2014) Real-time
440 measurements of the concentration and isotope composition of atmospheric and
441 volcanic CO₂ at Mount Etna (Italy). *Geophys Res Lett* 41:2382-2389,
442 doi:10.1002/2014GL059722

443 Rizzo AL, Liuzzo M, Ancellin MA, Jost HJ (2015) Real-time measurements of δ¹³C, CO₂
444 concentration, and CO₂/SO₂ in volcanic plume gases at Mount Etna, Italy, over 5
445 consecutive days. *Chem Geol* 411:182-191

446 Shinohara H (2005) A new technique to estimate volcanic gas composition: plume
447 measurements with a portable multi-sensor system. *J Volcanol Geotherm Res*
448 143:319-333

449 Vogel FR, Huang L, Ernst D, Giroux L, Racki S, Worthy DEJ (2013) Evaluation of a
450 cavity ring-down spectrometer for in situ observations of ¹³CO₂. *Atmos Meas Techn*
451 6:301-308

452 Zapata G JA, Calvache V ML, Cortés J GP, Fischer TP, Garzon V G, Gómez M D,
453 Narváez M L, Ordóñez V M, Ortega E A, Stix J, Torres C R, Williams SN (1997) SO₂
454 fluxes from Galeras volcano, Colombia, 1989-1995: progressive degassing and
455 conduit obstruction of a Decade volcano. *J Volcanol Geotherm Res* 77:195-208

456
457

458 Figure captions

459

460 Figure 1: Photograph of our Picarro G-1101-i analyzer, showing the data acquisition
461 module (DAS) on top and the power supply/vacuum pump module below. (a) Front end
462 of instrument. (b) Rear view. Together the two modules weigh ~34 kg and are similar in
463 size to a large desktop computer.

464

465 Figure 2. Daily variability of a CO₂ gas standard measured in the field. The CO₂
466 concentration range is 2000-2500 ppm, the reference isotopic value is 43.0 per mil, and
467 the two-sigma standard deviation is 0.50 per mil.

468

469 Figure 3: A series of gas samples and standards analyzed by our Picarro CRDS and by
470 gas-source mass spectrometry. The excellent agreement shows the high accuracy of the
471 CRDS system. The line is a best-fit linear regression through the data points.

472

473 Figure 4: Interference of H₂S on the δ¹³C value. A 1000 ppm CO₂ gas standard with δ¹³C
474 of -28.5 per mil is analyzed by the CRDS from ~1 to ~13 minutes elapsed time. The
475 isotopic signal is stable and accurate. By contrast, when 500 ppb H₂S is added to the CO₂
476 standard at ~21 minutes, the δ¹³C value becomes more negative, ranging in value from -
477 35 to -37 per mil. The baseline is not stable, becoming increasingly negative with time.

478

479 Figure 5: A ¼-inch diameter copper tube filled with copper filings that removes H₂S gas
480 prior to isotopic analysis of CO₂ by the CRDS.

481

482 Figure 6: A 1000-ml ALTEF gas sampling bag used to collect gases in the field. The bag
483 can be connected directly to the CRDS for isotopic analysis of the CO₂ if the
484 concentration is less than 3000 ppm, or if concentrated, the CO₂ can be diluted to
485 concentrations appropriate for analysis.

486

487 Figure 7: Apparatus used to remove CO₂ from air in the field. The canister is filled with
488 ascarite which removes the CO₂ by the reaction $\text{CO}_2 + 2\text{NaOH} \rightarrow \text{Na}_2\text{CO}_3 + \text{H}_2\text{O}$. Air is
489 pumped through the canister at a rate of 0.5 l/min, monitored by a flowmeter.

490

491 Figure 8: (a) 30 ml anaerobic culture tube treated with 5 µl HgCl₂ to prevent bacterial
492 growth (Oremland et al. 1987). A 50 ml gas sample is injected into the tube for later
493 analysis by gas source mass spectrometry. (b) 210 ml anaerobic media bottle used for
494 transporting CO₂ gas standards in the field.

495

496 Figure 9: Screen grab showing a sample being analyzed from 1436 to 1445 hours. The
497 first several minutes of the analysis are not used, as the CO₂ is shifting from background
498 room air to the sample. The sample is analyzed from 1438 to 1445 hours. The lower noise
499 level of the sample relative to the background results from the higher CO₂ concentration
500 of the sample.

501

502

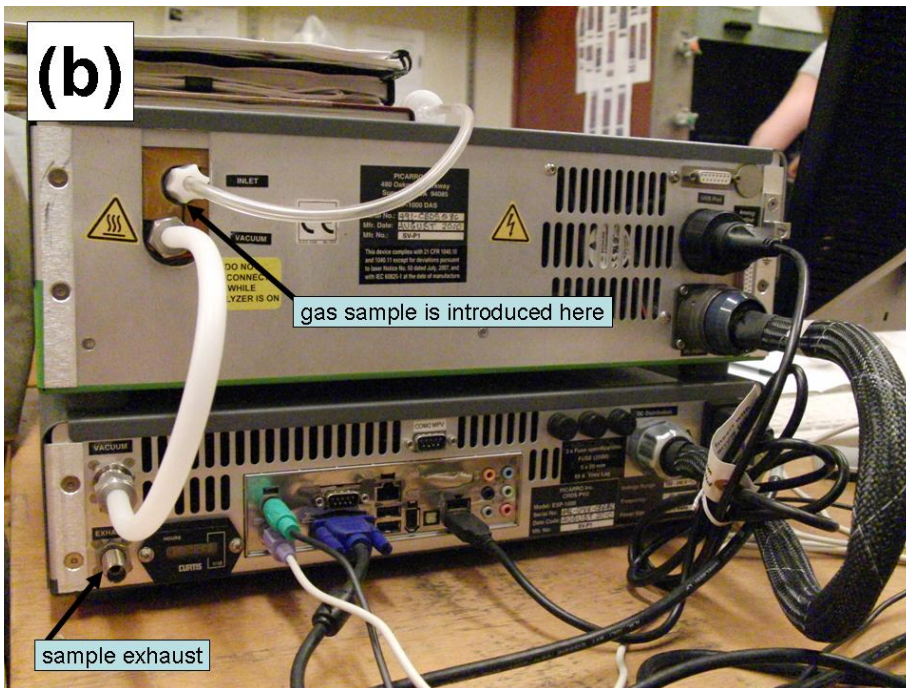
503

504



505

506



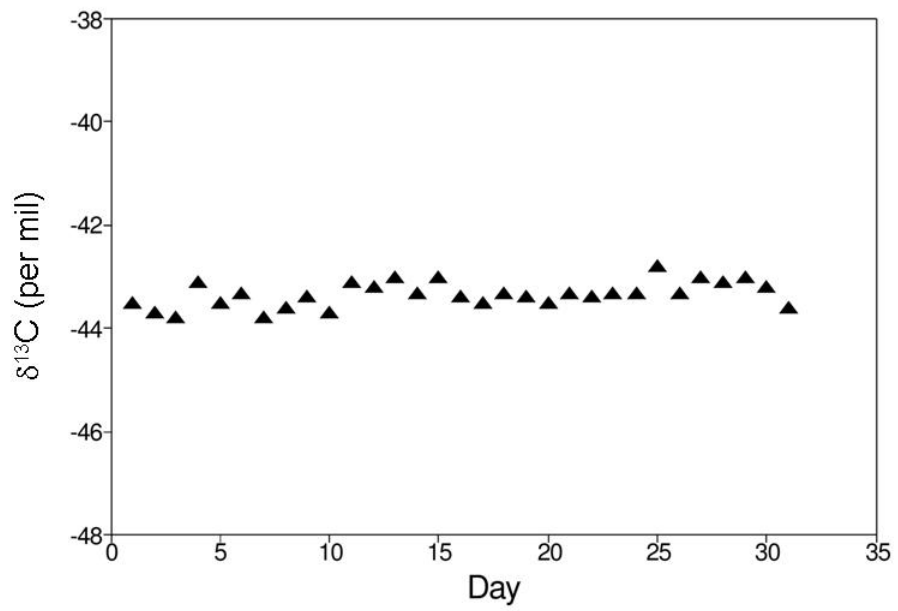
507

508

509

Figure 1

510
511
512
513
514
515



516
517
518
519
520
521

Figure 2

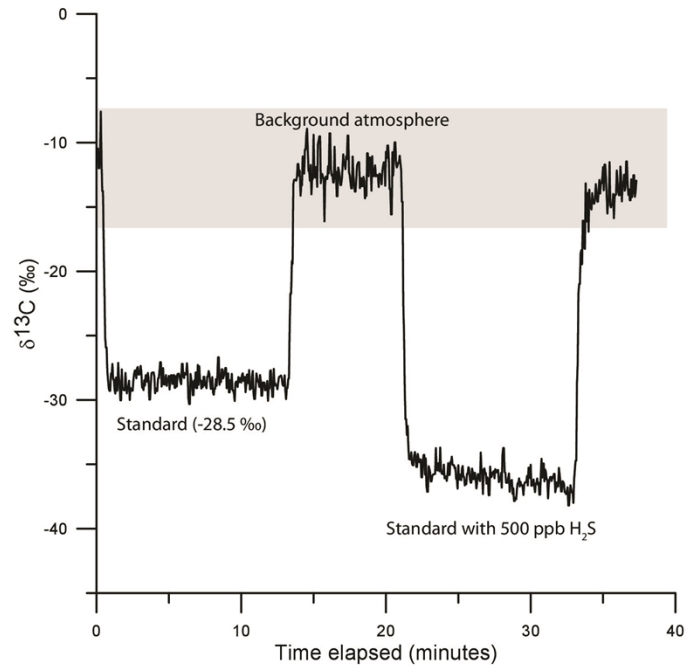


Figure 4

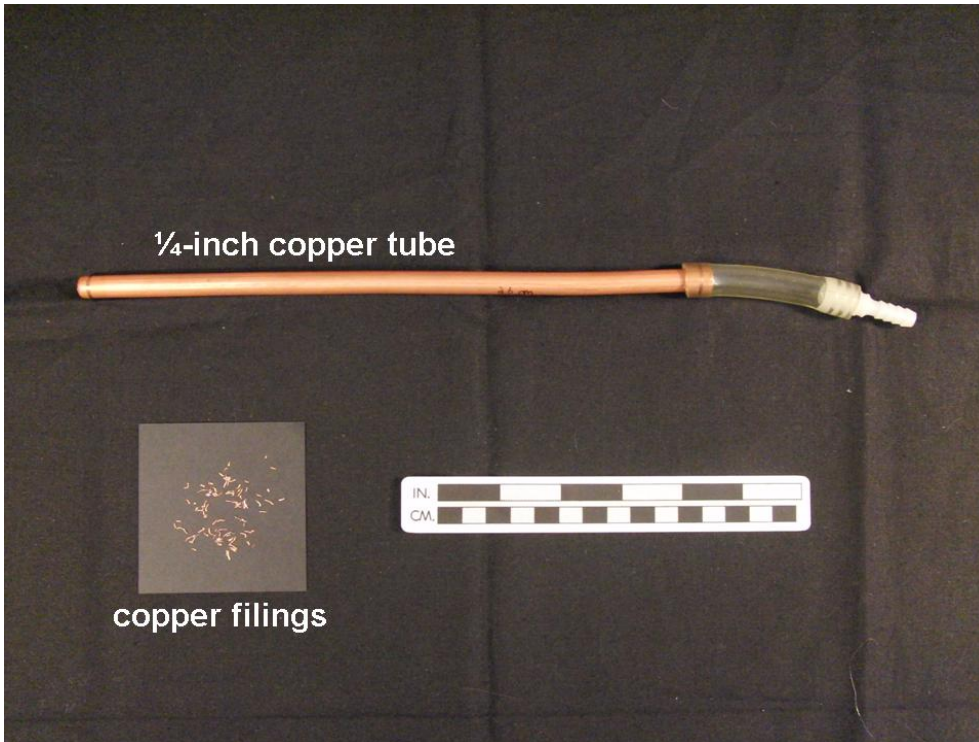
535

536

537

538

539



540

541

542

543

544

545

Figure 5

546

547

548

549

550

551

552

553

554



555

556

557

558

559

Figure 6

560

561

562

563

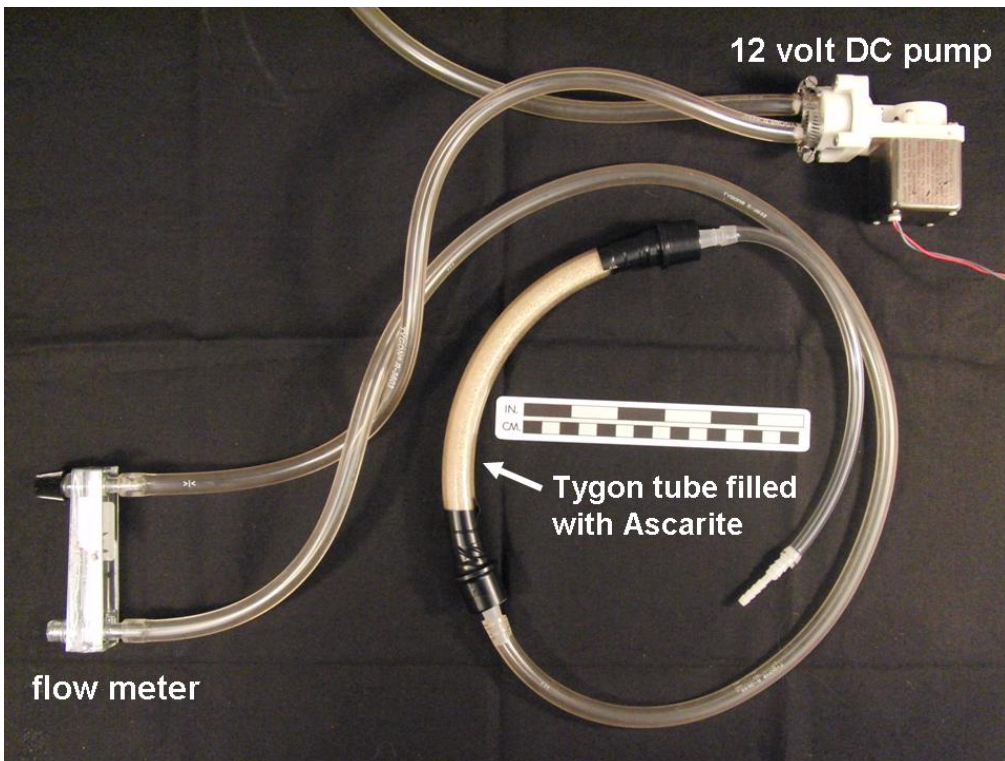
564

565

566

567

568



569

570

571

572

573

Figure 7

574

575

576

577

578

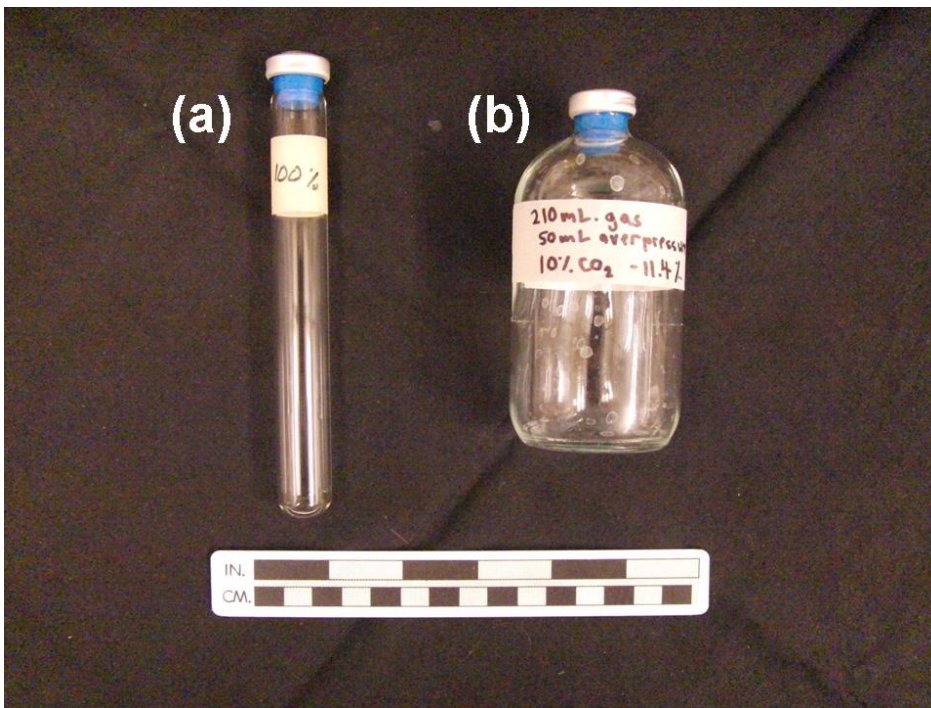
579

580

581

582

583



584

585

586

587

588

589

590

Figure 8

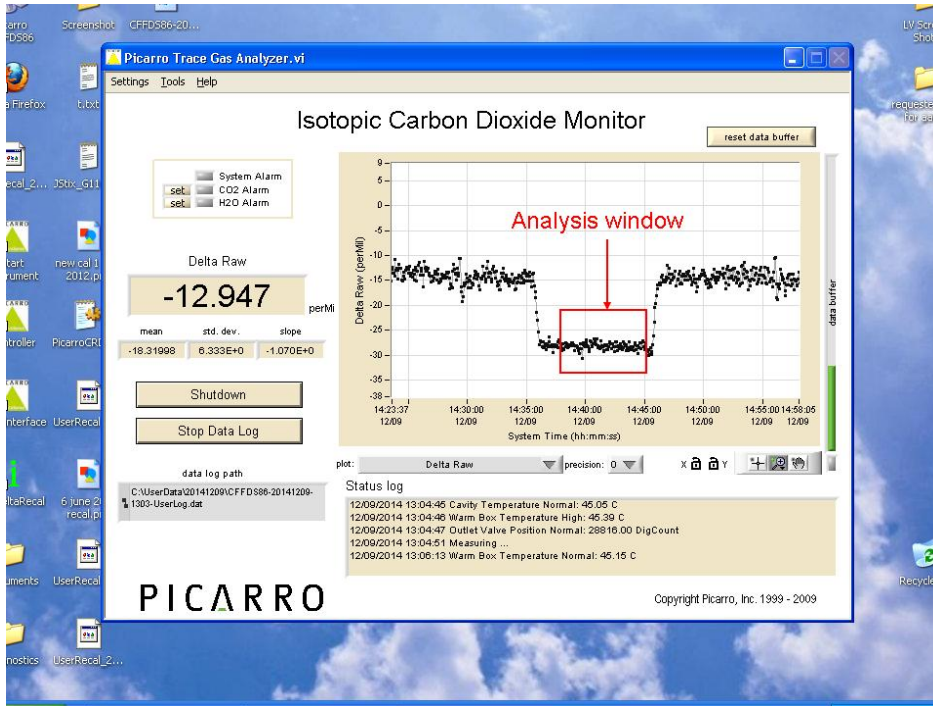
591

592

593

594

595



596

597

598

599

600

601

602

603

Figure 9